Electronic Supplementary Material (ESI) for Molecular Systems Design & Engineering.

Supplementary Information

Shape factors in the binding of soft fluorescent nanoshuttles with target receptor

Concetta Cozza,[1] Françisco M. Raymo[2]* and Adriana Pietropaolo[1]*

[1] Dipartimento di Scienze della Salute, Università di Catanzaro, Viale Europa, 88100 Catanzaro, Italy

[2] Laboratory for Molecular Photonics, Department of Chemistry, University of Miami, 1301 Memorial Drive, Coral Gables, FL 33146-0431, USA.

Contents

1.1 Binding between the soft nanoparticles and the folate receptor

We simulated the interactions between the folate receptor and the nanoparticle in order to predict and optimize the binding properties, as well as the factors that affect the binding. The coordinates of the human folate receptor alpha are deposited in the Protein Data Bank with the pdbcode 4LRH[1].
The nanoparticle under consideration is constituted by nine chains of the methacrylate copolymer, whose structure is reported in Figure 1a of the main text, in which the length of the PEG arm of the folate monomer was varied from 4 to 16 PEG units (section 1.2 reports the details of the enhanced sampling of the nanoparticles).
Steered Molecolar Dynamics (SMD)[2] simulations were preliminary performed in order to place the folate monomer belonging to the nanoparticle at the entrance of the binding site reported in the structure solved from X-ray crystallography. For this scope, the distances involving Asp81, Ser174, Arg106, Arg103 and His135 were used for guiding the binding, targeting those identified from X-ray diffraction data[1].
Afterwards, each conformation was minimized and then equilibrated at 300 K. Production runs were then carried out at 300 K with a time step of 2 fs.

The simulations were carried out in the framework of Parallel bias metadynamics[3], using as reaction coordinate a bespoke switching coordinate (i.e. *switch on/off*) based on the coordination number, s, described in eq. 1:

$$s = \sum_{i\in G_1}\sum_{j\in G_2} s_{ij}\ ;\ s_{ij} = \frac{1-\left(\frac{r_{ij}-d_0}{r_0}\right)^n}{1-\left(\frac{r_{ij}-d_0}{r_0}\right)^m}\ ;\ switch(on/off) = \frac{s_{i,j}}{max\left(s_{i,j}\right)} \qquad \text{S1)}$$

where r_{ij} are the pair distances $|\mathbf{r}_i\text{-}\mathbf{r}_j|$ of the atoms i,j belonging respectively to group G_1 and G_2, comprising the geometric centers of the two folate rings and the ones of Trp171 belonging to the binding pocket, with a cutoff of 6 Å[4]. We also biased the simulations on a second switching function in which G_1 comprises the NH group of the folate ring, the NH_2 amino group of the folate ring, contacting the oxygens of Asp81 of group G_2, the oxygen of Ser174 contacting the amide nitrogen and the carbonyl oxygen of the folate ring of group G_2, the guanidinium nitrogen of Arg106 and Arg103 both contacting the carbonyl oxygen of the folate ring of group G_2, the nitrogen of Trp138 and Trp140 both contacting the carboxyl group of the folate monomer of group G2.
After an initial sampling, we proceeded the simulations using the first switching function, owing to its capability in following the on/off switching mechanism and reaching free-energy convergence (Figures S4-S9).

An initial height of 1.2 kJ/mol with a sigma of 0.35 was applied using a bias factor of 25 in the framework of the multiple walker technique[5] using six replicas of bound and dissociated complexes. Free-energy convergence was assessed using the standard block-analysis techniques, following the protocol described in the PLUMED tutorial https://plumed.github.io/doc-v2.4/user-doc/html/trieste-4.html.

All the simulations were carried out with GROMACS v.2020.2[6] patched with PLUMED[7], version 2.7.0 with a total length of 0.75 μs. The CHARMM36 force field[8] was used for the protein and for the polymer, the CgenFF[9] for the folate derivative, together with TIP3P water model[10]. A stochastic thermostat[11] with a coupling time of 0.1 ps was used with LINCS constraints[12]. The particle-mesh Ewald method[13] was used for the electrostatic interactions. The systems were solvated in an octahedron box containing 202513 water molecules for M04-system, 212053 for M08-system and 232753 for M16-system. The net excess charge of the systems was neutralized adding 23 Na^+ ions.
Open data of the enhanced sampling simulations of fluorescent soft nanoshuttles binding folate receptor alpha are available in the PLUMED-NEST repository under Project ID: plumID:20.031 https://www.plumed-nest.org/eggs/20/031/ .

1.2 Conformational space exploration of the soft nanoparticles

Atactic random configurations of a 28-mer of the methacrylate copolymer reported in Figure 1a of the main text and based on [14] constitute the nanoparticle, in which the folate monomer size was varied with a length of 4,8,16 PEG units. The number of chains range from three to twenty. The CHARMM36 parameters[8] were used for the polymer, the CgenFF[9] for the folate derivative, together with the recently developed parameters for BODIPY[15] and the TIP3P potential[10] was used for water molecules, under GROMACS 2016 package[16] with Plumed 2.3.1[7]. Well-tempered[17] metadynamics[18] was used in the framework of multiple walkers[5] with a bias constructed adding every 1 ps a Gaussian function of an initial height of 2.5 kJ/mol. We simulated 36 walkers in NVT ensemble. A stochastic thermostat[11] with a coupling time of 0.1 ps was used. Periodic boundary conditions were applied and a 1.2 nm cutoff for Lennard-Jones and electrostatic interactions was used.

In order to guarantee a constant chemical potential we considered a box including two nanoparticles (i.e. having a total number of chains equal to the sum of the minimum and maximum chain length, in our case 23 in each box). The metadynamics potential was added only to one nanoparticle. Two nanoparticles for a total of 23 chains (176272 atoms) were solvated in a water box of size 48x22x22 nm^3 (2249916 atoms).

The relative positions of the monomers with respect to a director axis (i.e. the z-axis) were disclosed through the calculation of the second order parameter $\langle P_2 \rangle$ (equation 2) averaged among the orientations of the monomers. A value of $\langle P_2 \rangle$ equal to zero indicates isotropic orientations of the chains, which identifies a spherical shape.

$$\langle P_2 \rangle = \frac{1}{2}\langle 3cos^2(\theta) - 1 \rangle \qquad \text{S2)}$$

In addition, the hydrodynamic diameter (equations 3-5) was used as collective variables to identify also the nanoparticle sizes. It was calculated following the Flory theory of polymer solutions[19] as twice the radius of gyration scaled with a factor of $(5/3)^{1/2}$. The oxygen atoms belonging to the poly(ethylene glycol) side chains were taken into account since highly exposed to the water solvent.

$$\rho_k = \left(\frac{\sum_i^n m_{i,k}|\boldsymbol{r}_{i,k} - \boldsymbol{r}_{COMk}|^2}{\sum_i^n m_{i,k}}\right)^{\frac{1}{2}} \qquad \text{S3)} \qquad \boldsymbol{r}_{COMi,k} = \frac{\sum_i^n \boldsymbol{r} m_{i,k}}{\sum_i^n m_{i,k}} \qquad \text{S4)}$$

$$D_{H,k} = 2\rho_k \qquad \text{S5)}$$

$\mathbf{r}_{i,k}$ are the coordinates of the atom i belonging to the nanoparticle k, $\mathbf{r}_{COM\,k}$ are the coordinates of the center of mass encompassing the carbon atoms of the polymer main chain and the oxygens belonging to the poly(ethylene glycol) side chains and $m_{i,k}$ is the mass of the atom i belonging to the nanoparticle k.
The number of chains identifying each nanoparticles is followed through the calculation of the coordination number (s) estimated along the chain edge contacts. It is defined under equation (6):

$$s = \sum_{i\in G_1}\sum_{j\in G_2} s_{ij};\ s_{ij} = \frac{1-\left(\frac{r_{ij}-d_0}{r_0}\right)^n}{1-\left(\frac{r_{ij}-d_0}{r_0}\right)^m}\ r_0=3.0\ \text{nm};\ d_0=0 \qquad \text{S6)}$$

where r_{ij} are the pair distances $|\mathbf{r}_i\text{-}\mathbf{r}_j|$ of the atoms i,j belonging respectively to group G_1 and G_2, comprising the edge carbons of the polymer main chain, as well as the oxygens belonging to the poly(ethylene glycol) side chains.

Electronic CD and UV/VIS spectra calculations

The intrinsic rotatory strengths were calculated at the WB97XD/6-31G* level of theory including long-range corrections[20] as well as empirical dispersion[21], for the folate receptor and residues 134-136;170-171 constituting the alpha site of the human folate receptor and extracted from the free-energy minimum conformations having the lowest RMSD value with respect to the structure of human folate receptor alpha in complex with folate receptor[1]. ECD spectra calculations were run using Gaussian 16 package[22]. All the ECD spectra were calculated considering fifty singlet excited states at the WB97XD/6-31G*. Rotatory strengths are reported in the usual c.g.s. units of 10^{-40} esu.cm.erg/Gauss and calculated within the dipole-length formalism. The calculations of the ECD spectra at a given wavelength, λ, were done assuming Gaussian bands with 1000 cm^{-1} full width at half-height for all transitions centered at a given excitation wavelength. A factor of 2.278 was applied during the conversion of rotatory strengths and Δε values.[23] The calculations of electronic UV/VIS spectra were done in the same way, assuming the factor 2.8710^4 accounting for the conversion between oscillator strengths and the molar extinction coefficients.[21]

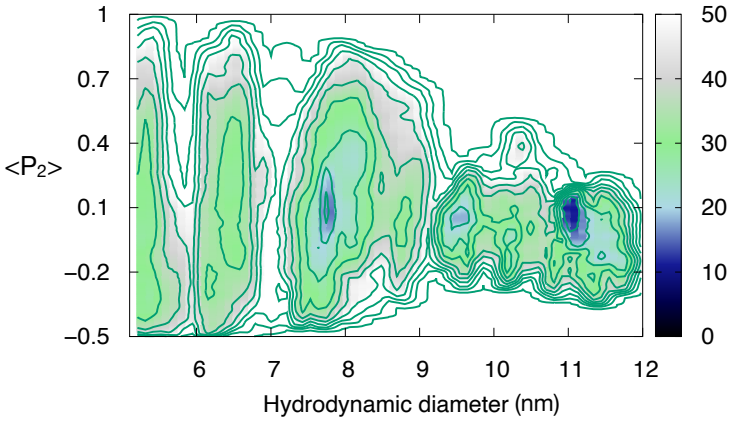

number of chains	hydrodynamic diameter (nm)	<P_2>
3	5.0	-0.4
4	5.5	-0.3
5	6.6	-0.3
6	7.0	-0.2
7	7.2	-0.1
8	7.4	0.0
9	7.5	0.0
10	8.0	0.0
11	9.0	0.2
12	9.5	0.2
13	10.0	0.1
14	11.0	0.0
15	9.8	0.1
16	11.0	0.2
17	11.3	0.2
18	11.3	0.2
19	11.3	0.2
20	12.0	0.3

Figure S1: Free-energy landscape as a function of the hydrodynamic diameter and the average second order parameter <P_2> reconstructed for the nanoparticle with the shortest PEG length (NP_04). The values of number of chains, hydrodynamic diameter and <P_2> are reported for each cluster of conformations corresponding to the lowest free-energy basins.

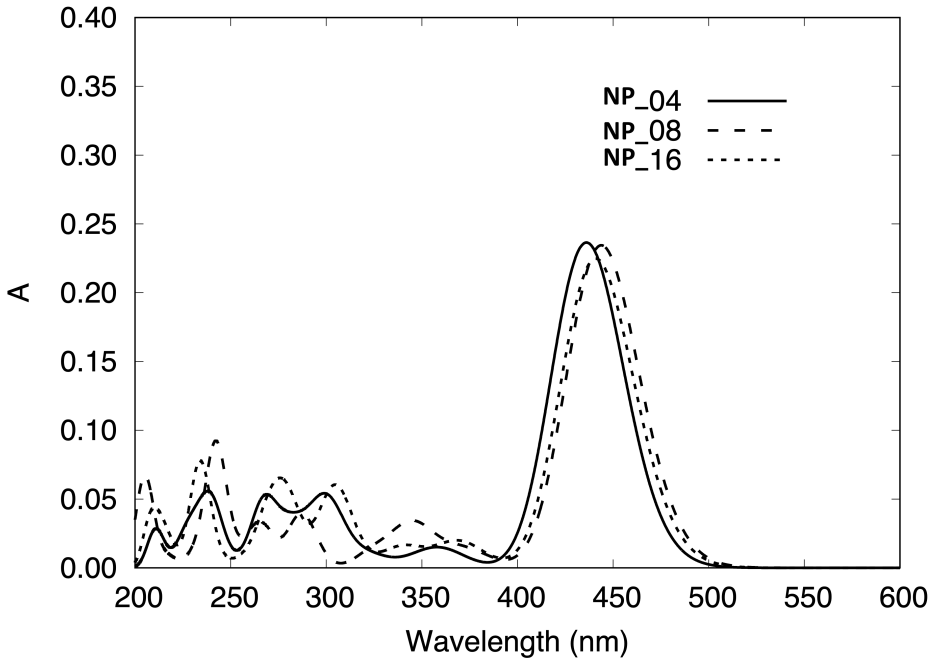

Figure S2: Calculated UV/VIS spectra for BODIPY conformers belonging to the nanoparticles (NP) with the folate monomer size ranging from 4 (NP_04), 8 (NP_08) and 16 (NP_16).

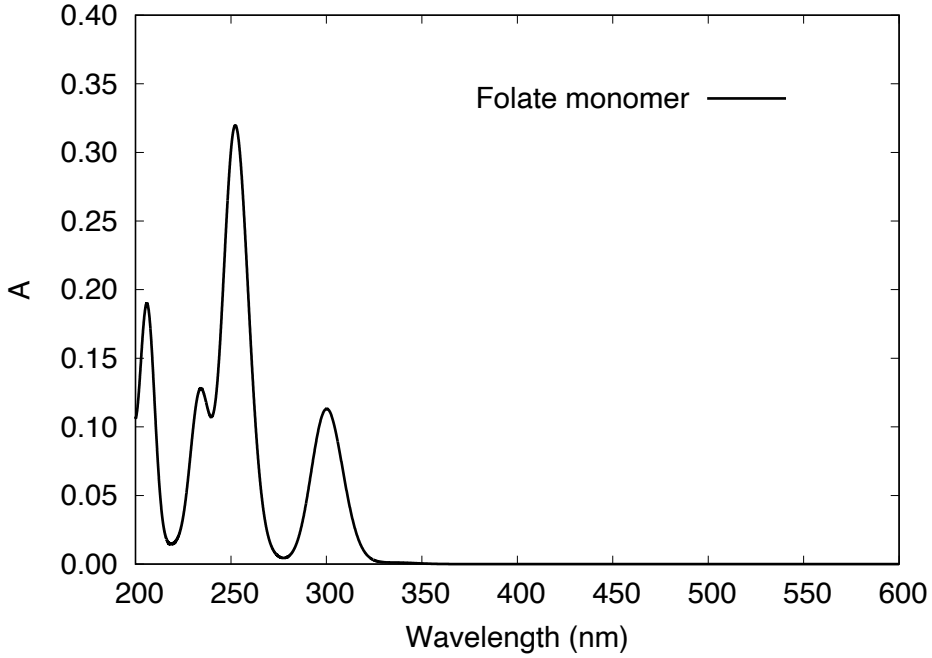

Figure S3: Calculated UV/VIS spectra for folate monomer belonging to the nanoparticle (NP) with the shortest PEG arm (NP_04).

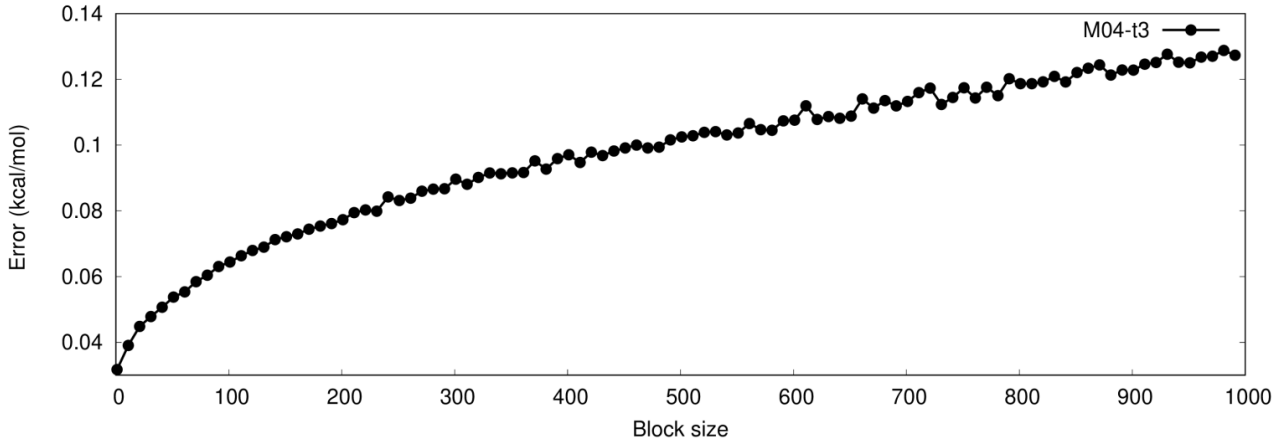

Figure S4: Block analysis of the simulation of M04-system.

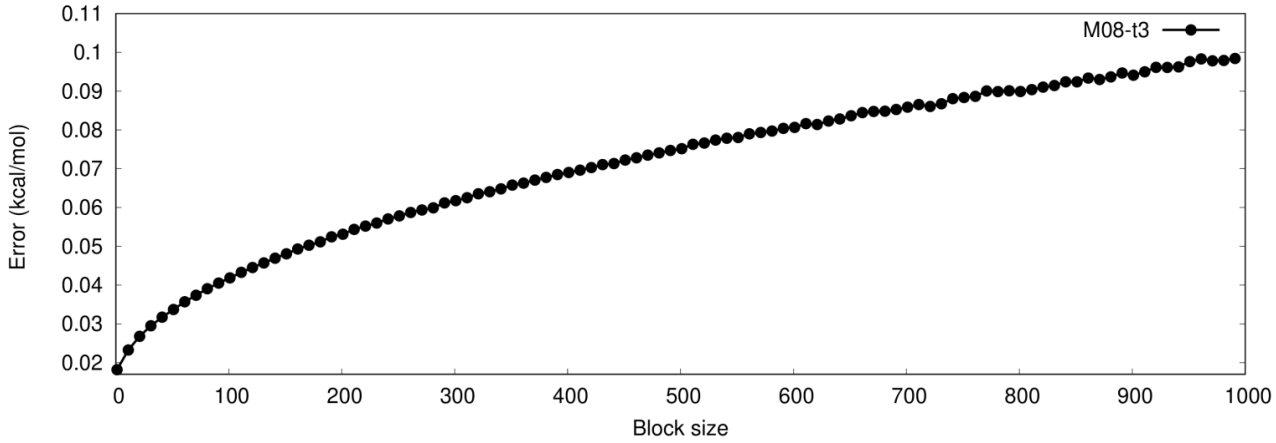

Figure S5: Block analysis of the simulation of M08-system.

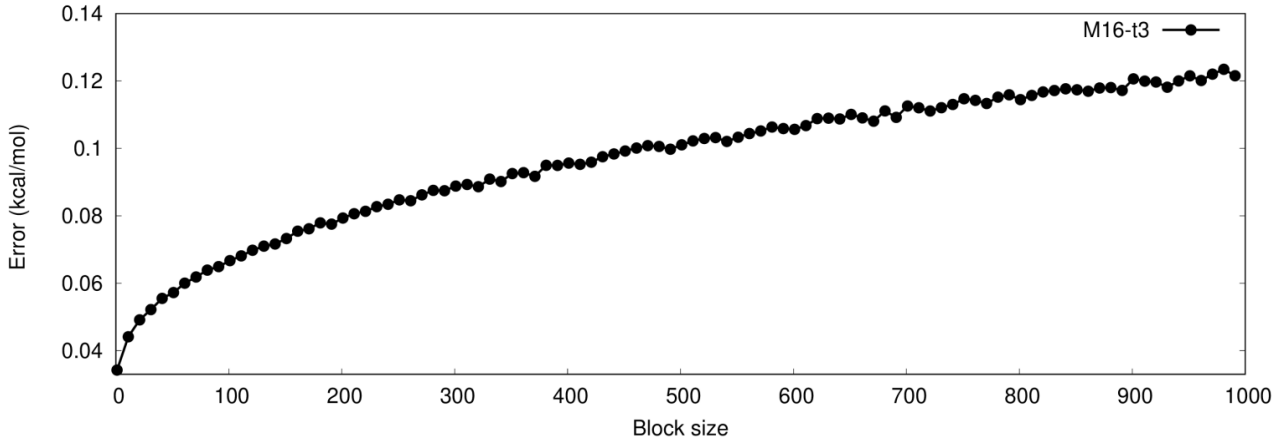

Figure S6: Block analysis of the simulation of M16-system.

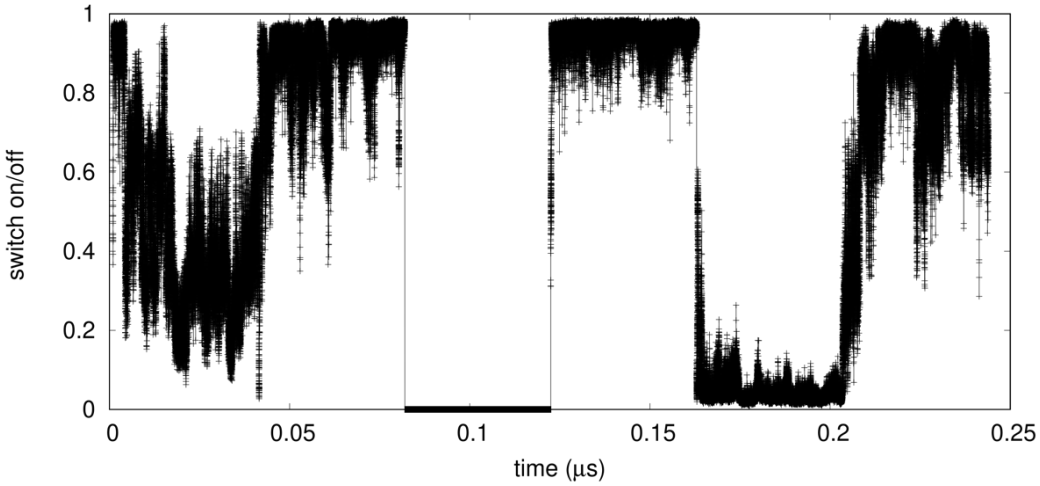

Figure S7: Variation of the switch on/off coordinate during the free-energy simulation for NP_04.

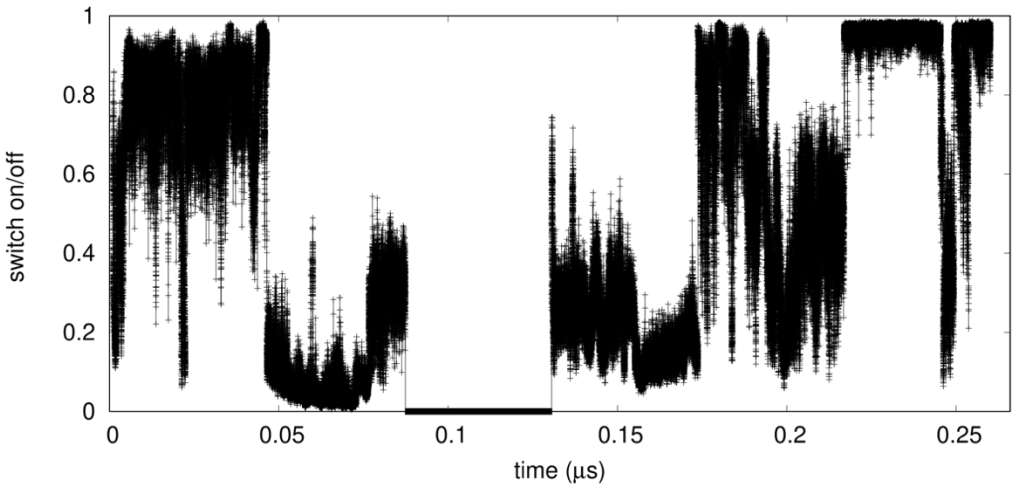

Figure S8: Variation of the switch on/off coordinate during the free-energy simulation for NP_08.

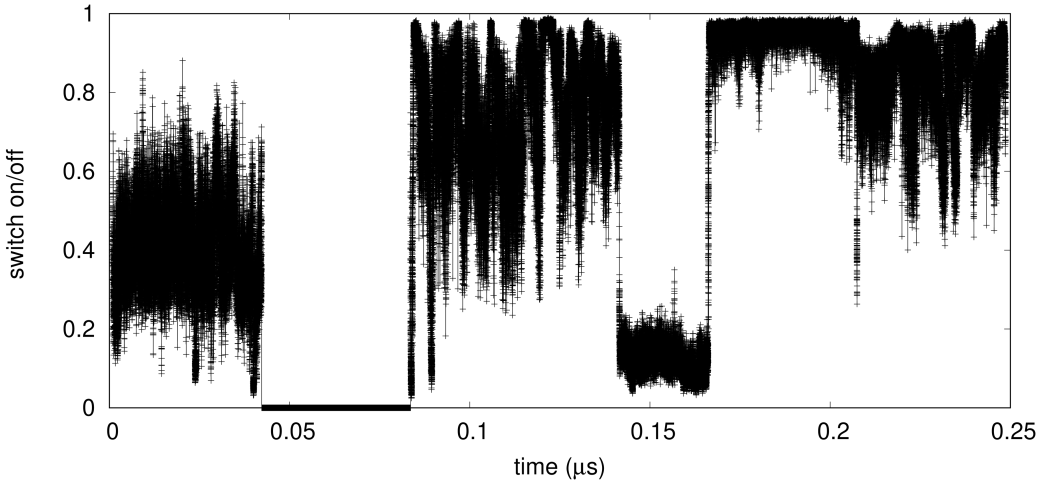

Figure S9: Variation of the switch on/off coordinate during the free-energy simulation for NP_16.

Table S1. Rotational strength predicted at the WB97XD/6-31G* level for the FR alpha site binding the NP_04.

443.0671	256.40
-75.7925	254.63
-12.2360	251.30
75.2910	239.30
-0.6373	229.90
56.3307	227.59
-12.7609	218.79
-4.6519	215.93
33.6234	215.74
140.6941	212.13
32.4799	208.75
-242.9207	204.73

Table S2. Rotational strength predicted at the WB97XD/6-31G* level for the FR alpha site binding the NP_08.

-393.5819	262.58
-356.5114	252.37
3.2461	245.43
-392.1112	242.89
103.4614	224.90
34.1836	221.63
-7.6209	220.26
53.6044	218.49
-36.5237	218.30
84.3364	216.78
9.1880	214.28
-482.4745	206.38
438.1243	203.54
135.0306	202.18

Table S3. Rotational strength predicted at the WB97XD/6-31G* level for the FR alpha site binding the NP_16.

588.9611	254.29
344.8734	248.22
22.0514	242.89
284.4418	238.57
-4.0441	236.03
55.5447	229.74
12.1516	221.38
-148.2958	220.70
8.4817	211.81
-10.3005	207.74
36.8541	205.45
187.3675	200.60

Table S4. Rotational strength predicted at the WB97XD/6-31G* level for the Folate monomer belonging to the NP_04.

-21.3100	336.20
291.6660	301.60
-287.7174	299.28
99.5723	273.89
17.7943	258.74
5.2763	256.26
2.9526	253.00
-3.9224	251.26
31.1052	248.41
76.8036	234.93
71.0999	231.53
-30.1504	231.39
27.2380	226.16
-166.3016	219.78
0.0679	217.95
23.2002	217.03
-10.9312	212.91
-36.9516	211.57
-458.0153	206.30
-1.4288	205.21

Table S5. Rotational strength predicted at the WB97XD/6-31G* level for the Folate monomer belonging to the NP_08.

-353.4234	309.70
501.0625	296.32
74.7201	279.90
-334.0493	259.48
671.1551	251.46
-229.0939	248.25
13.7085	243.23
21.7426	240.27
47.9640	239.50
-374.2334	237.06
-224.5026	233.87
22.5941	230.74
-4.4170	224.36
142.1035	222.71
-64.4158	219.13
59.1002	216.34
123.7270	215.06
1.3621	213.08
68.2279	212.75
-87.1176	208.99
-244.8824	205.71
315.7121	205.43

Table S6. Rotational strength predicted at the WB97XD/6-31G* level for the Folate monomer belonging to the NP_16.

-32.6529	317.35
-232.3030	291.59
40.6441	287.99
-55.5363	264.98
-502.9688	262.56
31.2770	245.76
118.1554	245.57
29.9967	245.46
256.5946	243.57
77.1806	240.57
-15.0286	236.46
-358.6715	233.19
57.1702	231.53
9.1900	225.63
53.1412	225.03
71.9708	224.06
213.9379	222.86
-1.0284	219.74
93.3171	216.69
-3.5346	215.32
-40.9977	213.34
-250.4822	208.91
-44.1188	208.80

References

1. C. Chen, J. Ke, X.E. Zhou, W. Yi, J.S. Brunzelle, J. Li, E.-L. Yong, H.E. Xu, K. Melcher. *Nature,* 2013, 500, 486–489.

2. P.E. Marszalek, H. Lu, H. Li, M. Carrion-Vazquez, A.F. Oberhauser, K. Schulten, J.M. Fernandez. *Nature,* 1999, 402, 100-103.

3. J. Pfaendtner, M. Bonomi. *J. Chem. Theory Comput.,* 2015, 11, 5062-5067.

4. D.B. Ninković, G.V. Janjić, D.Ž. Veljković, D.N. Sredojević, S.D. Zarić. *ChemPhysChem,* 2011, 12, 3511–3514.

5. P. Raiteri, A. Laio, F.L. Gervasio, C. Micheletti, M. Parrinello. *J. Phys. Chem. B,* 2006, 110, 3533-3539.

6. E. Lindahl, M. Abraham, B. Hess, D. van der Spoel. (2020, April 30). GROMACS 2020.2 Source code (Version 2020.2). Zenodo. http://doi.org/10.5281/zenodo.3773801

7. M. Bonomi et al. The PLUMED consortium. *Nat. Methods,* 2019, 16, 670–673.

8. R.B. Best, X. Zhu, J. Shim, P.E.M. Lopes, J. Mittal, M. Feig, A.D. MacKerell Jr. *J. Chem. Theory Comput.,* 2012, 8, 3257-3273.

9. K. Vanommeslaeghe, E. Hatcher, C. Acharya, S. Kundu, S. Zhong, J. Shim, E. Darian, O. Guvench, P. Lopes, I. Vorobyov, A.D. Mackerell Jr. *J. Comput. Chem.,* 2010, 31, 671-690.

10. W.L. Jorgensen, J. Chandrasekhar, J.D. Madura, R.W. Impey, M.L. Klein. *J. Chem. Phys.,* 1983, 79, 926.

11. G. Bussi, D. Donadio, M. Parrinello. *J. Chem. Phys.,* 2007, 126, 014101.

12. B. Hess. *J. Chem. Theory Comput.,* 2008, 4, 116-122.

13. U. Essmann, L. Perera, M.L. Berkowitz, T. Darden, H. Lee, L.G. Pedersen. *J. Chem. Phys.* 1995, 103, 8577-8593.

14. S. Tang, Y. Zhang, E.R. Thapaliya, A.S. Brown, J.N. Wilson, F.M. Raymo. *ACS Sensor,* 2017, 2, 92-101.

15. I. Pochorovski, T. Knehans, D. Nettels, A.M. Müller, W.B. Schweizer, A. Caflisch, B. Schuler, F. Diederich. *J. Am. Chem. Soc.,* 2014, 136, 2441-2449.

16. B. Hess, C. Kutzner, D. van der Spoel, E. Lindahl. *J. Chem. Theory Comp.,* 2008, 4, 435-447.

17. A. Barducci, G. Bussi, M. Parrinello. *Phys. Rev. Lett.,* 2008, 100, 020603.

18. A. Laio, M. Parrinello. *Proc. Natl. Acad. Sci. USA,* 2002, 99, 12562-12566.

19. I. Teraoka. Polymer solutions. An Introduction to Physical Properties, John Wiley & Sons, Inc., 2002.

20. J.D. Chai, M. Head-Gordon. *Phys. Chem. Chem. Phys.,* 2008, 10, 6615-6620.

21. S. Grimme. *J. Comput. Chem.,* 2006, 27, 1787-1799.

22. M.J. Frisch, G.W. Trucks, H.B. Schlegel, G.E. Scuseria, M.A. Robb, J.R. Cheeseman, et al. Gaussian 16 Rev. C.01, 2016, Gaussian 16 Rev C01.

23. N. Berova, K. Nakanishi, R.W. Wood. (Eds.). Circular Dichroism: Principles and Applications, 2nd edR, Wiley-VCH, New York, 2000, 877.